

# Experimental Realization of Nd-YAG Laser

Ashish Panigrahi

School of Physical Sciences,  
National Institute of Science Education and Research, Bhubaneswar

This is an abstract.

## INTRODUCTION

**LASER** stands for Light Amplification by Stimulated Emission of Radiation. It is a source of highly directional and intense light, with the emitted radiation being monochromatic and coherent in nature.

In our discussion, we shall deal with a particular type of laser called Neodymium Yttrium Aluminium Garnet (Nd-YAG) laser. This laser has various medical and scientific applications especially in spectroscopy and surgery. Here, we shall discuss the working principle of a general laser and Nd-YAG laser in particular. Afterwards, the experiment along with the relevant setup is described and results inferred.

## EXPERIMENTAL SETUP

Here, we proceed to describe the setup of our experiment consisting of various optical elements, an optical rail for their subsequent placement.

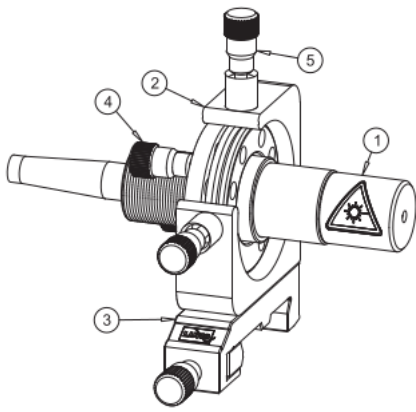


FIG. 1. Diode Laser (Module A)

**Diode Laser (Module A):** This module contains a diode laser with an emission spectrum containing 808 nm (1) light. The corresponding power is maximum at 20° C with a value of 500 mW. It is controlled via a *Peltier's element* which controls the injection current and temperature of the laser. As shown in fig. 1, it is attached to the adjustment holder (2) which is further attached to the carrier (3). This helps us fix the laser onto the optical rail.

In our setup, the temperature can be varied between 15° C and 35° C. The fine precision pitch screws (4 & 5) are used to micro-adjustments in order to align the optical

axis of the diode laser with the overall mechanical axis of the optic rail.

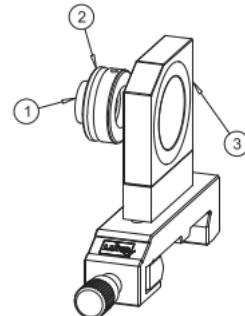


FIG. 2. Collimator (Module B)

**Collimator (Module B):** This module contains a collimator unit whose main task is to supply a parallel beam of light from the original divergent beam originating from the diode laser. It (1) consists of a three-lens system housed within a body with a large aperture and a focal length of 8 mm. It is mounted onto the holder (2) as shown in fig. 2. The holder is then fixed onto the optic rail of the setup.

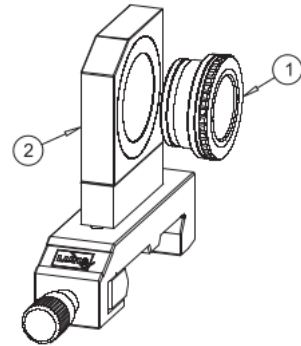


FIG. 3. Focussing Unit (Module C)

**Focussing Unit (Module C):** Shown in fig. 3, this module consists of a focussing unit needed to focus the collimated beam of light originating from the collimator onto the crystal (which is to be mounted onto module D). The lens (1) has a focal length of 60 mm and is mounted onto a 25 mm click holder (2). This is further placed and fixed on the optic rail of the setup.

**Adjustment Holder (Module D):** Shown in fig. 4, this module contains an adjustment holder (3) for housing the Nd:YAG crystal (2) onto an exchangeable mount (1). The crystal itself is polished on one of its

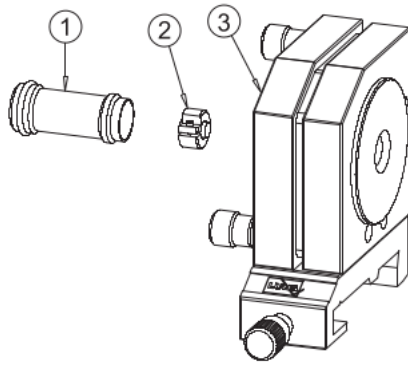


FIG. 4. Adjustment Holder (Module D)

ends to form a plane-parallel mirror. This polished coating is highly reflective for the emergent wavelength of light (1064 nm) and hence forms the left resonator of the entire optical cavity (to be mounted subsequently). This polished end of the crystal is placed to face the focussing unit. This mirrored coating is such that it is transparent to the 808 nm emission from the diode laser. The other end of the crystal is coated with an anti-reflection layer for 1064 nm light in order to keep the losses in the resonator cavity low. This end is also coated with a highly reflective layer for 532 nm light, in order to allow the outward propagation of corresponding green light out of the resonator cavity for the second harmonic generation experiment.

The crystal is placed in the exchange mount, which is mounted onto the corresponding adjustment holder. This is then fixed onto the optic rail. The fine adjustment screws help in aligning the resonator mirror in a way that the common optical axis of positioned perpendicularly to the mirrors.

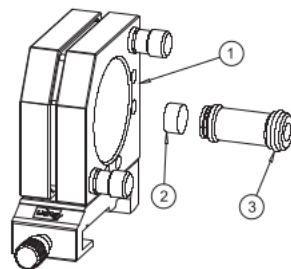


FIG. 5. Adjustment Holder with resonator mirror (Module E)

**Holder & Resonator Mirror (Module E):** Similar to module D, this contains a second resonator mirror (2) to form the overall cavity resonator. As shown in fig. 5, the mirror is placed inside a structure (3) which is then screwed onto the holder (1). This mirror has a spherical structure and is highly reflective, with a radius of curvature of roughly 100 mm.

**Filter plate holder (Module F):** In this module, two different filters depending on the experiment being

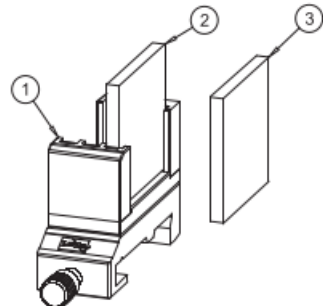


FIG. 6. Filter plate holder (Module F)

performed i.e. RG1000 and BG39. The former filters out 808 nm light which is sent as input to the whole setup. The latter filter only allows light of 532 nm wavelength to pass through. The corresponding module is shown in fig. 6.

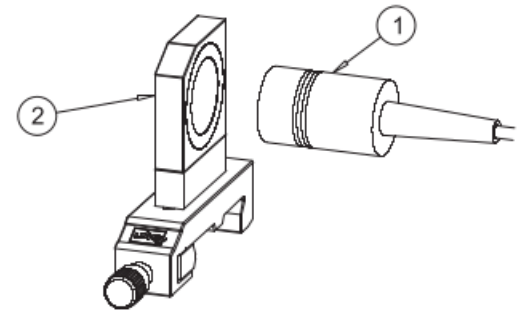


FIG. 7. Photodetector (Module G)

**Photodetector (Module G):** This module consists of a silicon-PIN photodetector (1) with a holder (2). This detector is then connected to a signal conditioner box, which allows the corresponding photodetector signal to be observed on an oscilloscope. The corresponding module is shown in fig. 7.



FIG. 8. Signal conditioner box

**Signal Conditioner Box:** This component allows for the signal from the photodetector to be fed onto the oscilloscope. This is achieved by converting the measured photodetector current (corresponds to the number of photons incident on the photodetector) to voltage. This apparatus is driven via a 9V battery. The

impedance can be tuned from  $50 \Omega$  to  $100 \text{ k}\Omega$ . The “OFF” position gives a high sensitivity using a  $1 \text{ M}\Omega$  shunt resistance. The fast signals, the lower shunt resistance value is used. The corresponding unit is depicted in fig. 8.



FIG. 9. Peltier’s element controller

**Peltier’s Element Controller:** This component is a completely digital device which allows the user to control the supplied injection current and temperature of the diode laser. The laser diode and the device is connected via a multi-pin connector. The injection current can be adjusted to a maximum value of 1000 mA. The range of temperature control is between  $15^\circ \text{ C}$  and  $35^\circ \text{ C}$ . The corresponding unit is depicted in fig. 9.

## EXPERIMENTS PERFORMED

During our hands-on experimental demonstration of the Nd:YAG laser, we performed several experiments. The details for the same are subsequently provided.

### Absorption Spectrum of Diode Laser

During this experiment, the objective is to determine the wavelength of the diode laser beam as a function of diode temperature and supplied injection current. From the energy level diagram of  $\text{Nd}^{3+}$  ions (see fig. 10), we see that there are four absorptions peaks at wavelengths 804.4 nm, 808.4 nm, 812.9 nm and 817.3 nm. All of these peaks are observed between a temperature range of  $0^\circ \text{ C}$  and  $60^\circ \text{ C}$ . However, our setup only allows temperature tuning in the range  $15^\circ \text{ C}$  to  $35^\circ \text{ C}$ .

**Setup:** For measuring the absorption spectra, we only need modules A through D, along with the photodetector. Note that we do not require an optical cavity for this case since we not observing any property related to the lasing action of the Nd:YAG crystal.

**Results:** In order to measure the spectra, we fixed the value of injection current and slowly varied the diode laser temperature. We measured the corresponding voltage vs temperature for injection current values 400 mA, 500 mA, 600 mA and 700 mA as shown in fig. 12. We also measured for injection currents 200 mA and

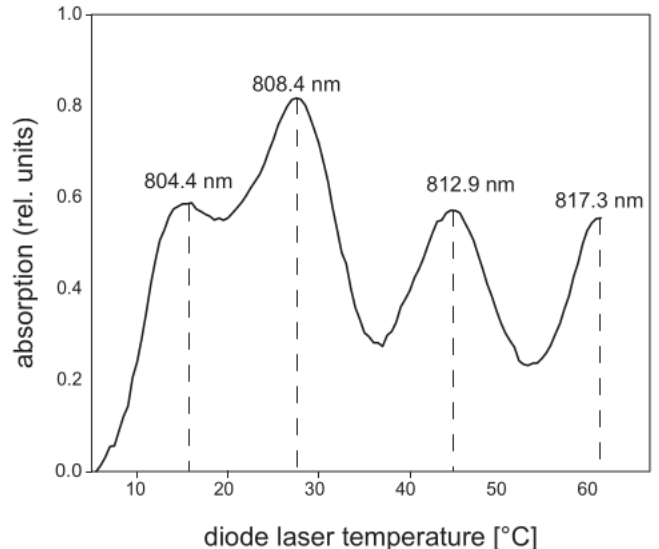


FIG. 10. Energy level diagram of  $\text{Nd}^{3+}$  ions.

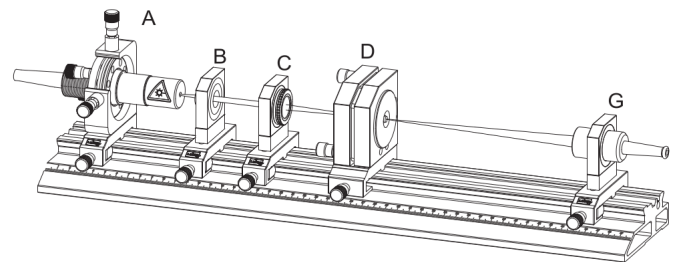


FIG. 11. Experimental setup for observing absorption spectra of  $\text{Nd}^{3+}$ .

300 mA (see fig. 13) but with lesser impedance value for greater sensitivity. The observed peak corresponds to a wavelength of 808.4 nm.

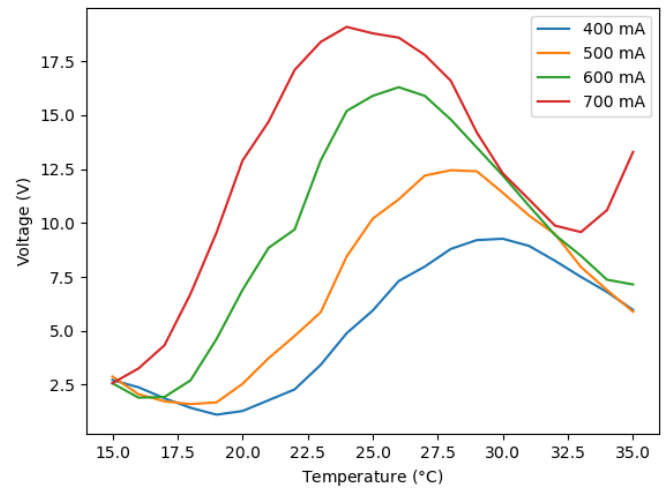


FIG. 12. Absorption spectra seen for injection current values 400 mA - 700 mA.

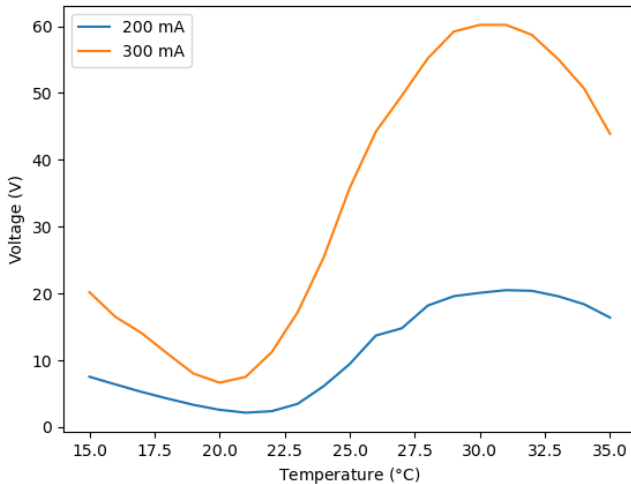


FIG. 13. Absorption spectra seen for injection current values 200 mA and 300 mA.

From fig. 12, we see that the position of the absorption peak shifts towards lower temperatures with increasing injection current. As seen from the plot, the output of the diode laser at 700 mA injection current is maximum at around 23° C.

#### Wavelength and temperature dependence

As seen from fig. 12 in our previous experiment, the absorption peaks at a certain value of diode temperature. The goal is to operate the diode laser such that this absorption peak is maintained and hence the wavelength remains constant (at a value of 808.4 nm). Plotting the corresponding variation of the injection current with temperature using data obtained from the absorption spectra, we observe a linear relation as shown in fig. 14.

This constant wavelength of 808.4 nm is used throughout all our experiments. The wavelength here remains constant from the simple concept of proportionality where with an increase in wavelength will be seen due to increase in temperature but at the same time a decrease is seen with decrease in injection current.

#### Power of Laser Diode

The objective here is to determine the output power of the diode laser as a function of diode temperature and injection current.

**Setup:** The setup remains the same as fig. 11 except that here, we also add an RG1000 filter after module D. In addition, since we are interested in determining the output power, a photodetector does not allow such

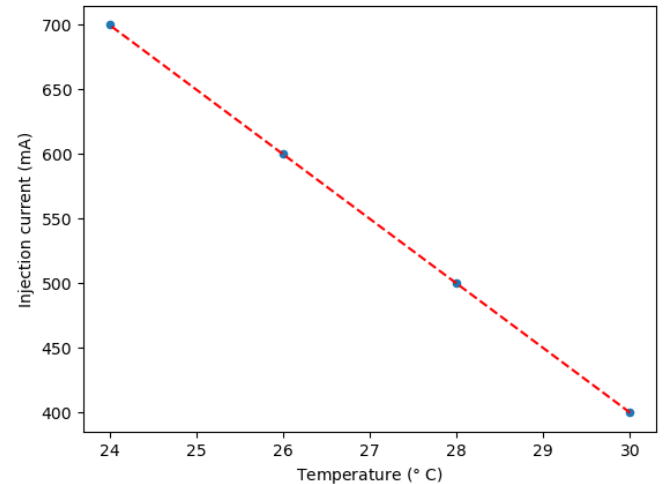


FIG. 14. Plot of injection current as a function of temperature at a constant wavelength of 808.4 nm.

measurement and thus we employ a optical power meter for the same. Once again, since we are interested to determining these parameters for the diode laser and not the Nd:YAG laser, setup of the cavity resonator is not done.

**Results:** For a fixed temperature, we first measure and observe the variation of output power as a function of injection current. This is done at two temperature values i.e. 20° C and 28° C.

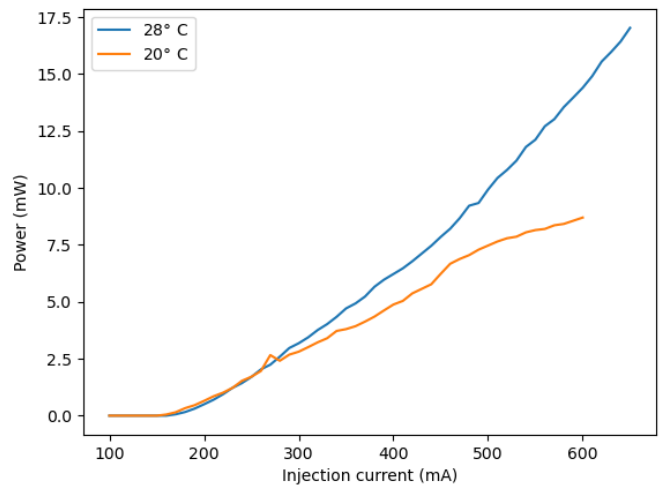


FIG. 15. Output power of laser diode as a function of injection current at various temperatures.

Subsequently, we also measure and observe the output power variation as a function of temperature at fixed values of supplied injection currents.

From the above plots, let us make certain inferences. From fig. 15, the output power varies approximately

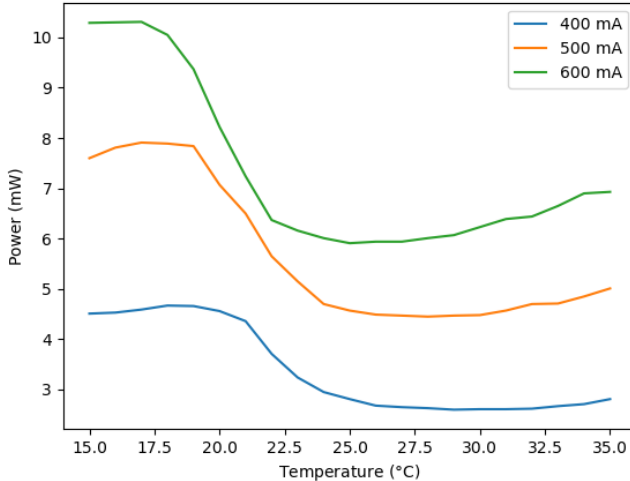


FIG. 16. Output power of laser diode as a function of temperature at various injection current values.

in a linear fashion with injection current. It is also observed that this linear increase in power is seen only after the injection current crosses a threshold value, which from the data obtained (and hence in fig. 15) is at  $(160 \pm 10)$  mA. Below this threshold, the output power is negligible.

In fig. 16, it is seen that the output power achieves a maximum at lower temperature but falls afterwards at various temperatures depending on the supplied injection currents i.e. the fall is seen at lower temperatures for measurements corresponding to higher injection currents. This particular trend is also seen in fig. 12, and hence consistency in our data is also verified.

The laser diode operation for subsequent experiments is done at a temperature of  $20^\circ$  C with an injection current value of 600 mA.

### Lifetime of ${}^4F_{3/2}$ level

Before the midsem, we discussed about the theory of lasing in Nd:YAG four-level system where the lasing transition corresponds to a stimulated emission from the metastable  ${}^4F_{3/2}$  state. This transition is radiative and corresponds to a wavelength of 1064 nm.

The lifetime of a state is defined as the time taken for the initial intensity (after pump source is switched off) to reduce to  $1/e$  fraction of its original intensity. Since lasing (for which population inversion is required) occurs from this level, the corresponding lifetime is expected to be longer than that of other energy states. From literature, the lifetime of  ${}^4F_{3/2}$  is  $250\ \mu s$ .

We then measure this lifetime using the oscilloscope as shown in fig. 17. The observed lifetime is measured

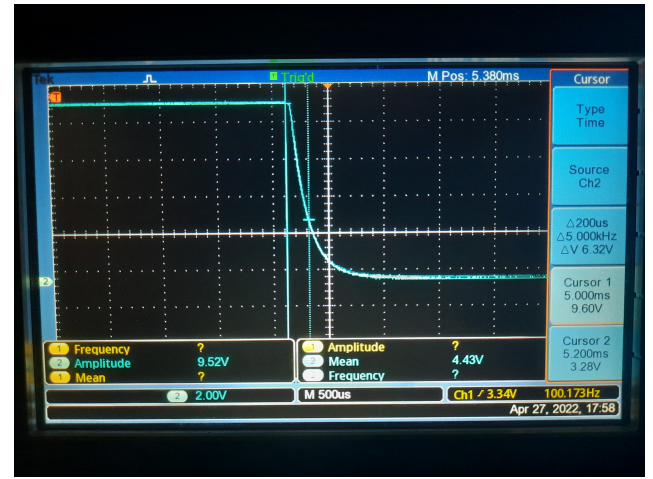


FIG. 17. Oscilloscope under cursor reading mode, displaying the measurement for the lifetime of  ${}^4F_{3/2}$  state.

to be about  $200\ \mu s$ . This value is quite erroneous compared to the literature value. A possible reason for this discrepancy can be due to the fact that after aligning our apparatus in order to achieve lasing, we performed the lifetime experiment after about 2 weeks, during which dust among other atmospheric particles may have deposited onto the surface of the Nd:YAG crystal, due to which an accurate reading for the lifetime was not observed.

### Spiking

In order to observe the phenomena of spiking, we proceed to setup the lasing component of the Nd:YAG laser setup.

### Theory:

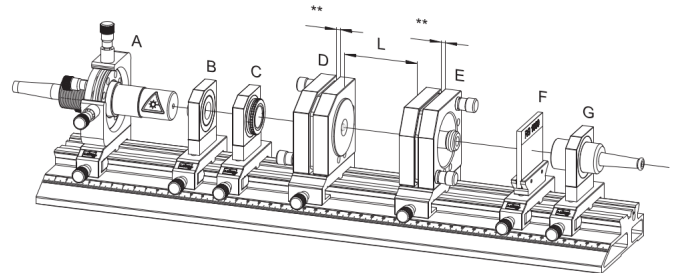


FIG. 18. Setup for lasing of Nd:YAG crystal.

**Setup:** All the modules previously discussed in the section on experimental setup, is used here. To achieve lasing, it is extremely important to carefully align the optical axis of the components with the mechanical axis of the optic rail. Without this it is impossible to achieve lasing action. Once lasing is achieved, we observe sparks between the two mirrors forming the resonator cavity i.e. between modules D and E. After placing the RG1000 filter and a special IR card behind it, we observe

light of 1064 nm being emitted from the cavity.

**Demonstration of Spiking:** We are able to directly observe laser spiking from the output of the oscilloscope. However, since the signal is fast, it is required that the impedance is setup to a value of 50 k $\Omega$ .



FIG. 19. Spiking as seen from an oscilloscope.

Note that there is a time lag, between the point when the laser diode is switched on and the first peak of the spike. This time difference is measured as a function of injection current at a temperature of 20° C and the corresponding data is plotted.

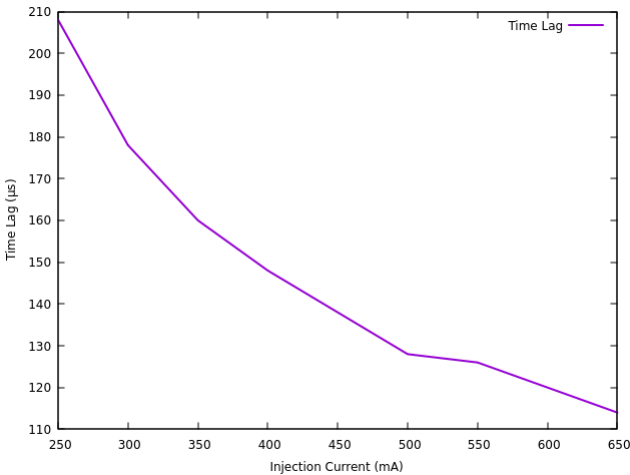


FIG. 20. Time lag measurement between the time when the laser diode is switched on and the first peak of the spike as a function of injection current at 20° C.

As seen from fig. 20, the time difference decreases with increasing injection current.

### Second Harmonic Generation

Often called SHG, second harmonic generation is a second-order nonlinear process. Conceptually, it means that after supplying a pump light source of frequency

$\omega$  through a nonlinear  $\chi^{(2)}$  crystal, the obtained light which emerges has a frequency of  $2\omega$ . In order to achieve this experimentally, we require a nonlinear optical element in our current setup. Here, a KTP crystal (Potassium Titanyl Phosphate) is used since it exhibits  $\chi^{(2)}$  nonlinearity. This element is inserted inside the optic cavity along with the original Nd:YAG crystal.

**Setup:** An additional holder is required to house the KTP crystal, for which module K is used as shown in fig. 21.

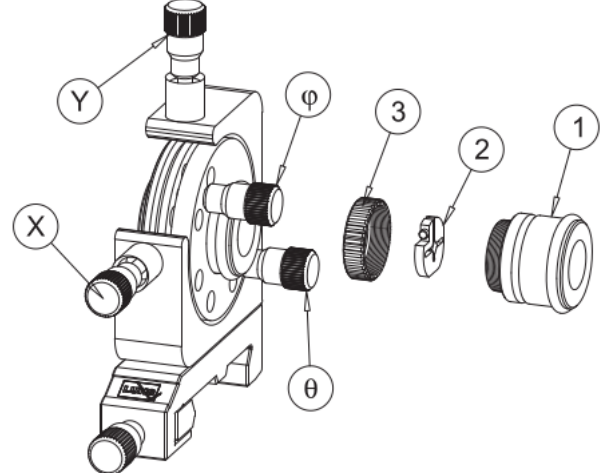


FIG. 21. Adjustment holder for KTP crystal (Module K)

Since the frequency is doubled, the corresponding wavelength reduces to half its original value after passing through the KTP crystal i.e. second harmonic of 1064 nm light, which is 532 nm. The crystal is inserted in (2) and then onto a holder (1), which is then fixed in place via a screw cap (3). The fine and coarse pitch screws ( $\varphi$ ,  $\theta$  and X, Y respectively) are used to tune the position of the crystal with respect to the optical axis of the setup.

The entire module K is then housed within the resonator cavity as shown in fig. 22. Note that instead of RG1000 filter, in this case we employ the BG39 filter to only allow 532 nm light to pass through.

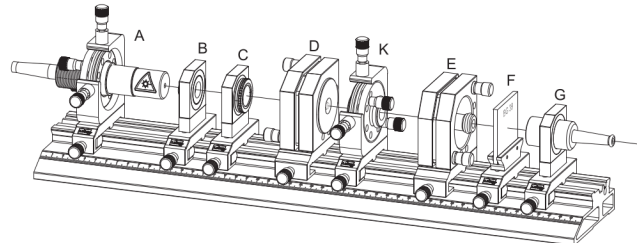


FIG. 22. Setup for performing the SHG experiment.

**Results:** We measured the output power of original lased light of 1064 nm, and then during SHG, we measured the corresponding output power of 532

nm light. Both the data were compared and the corresponding plot between SHG power output and fundamental power output is plotted in fig. 23.

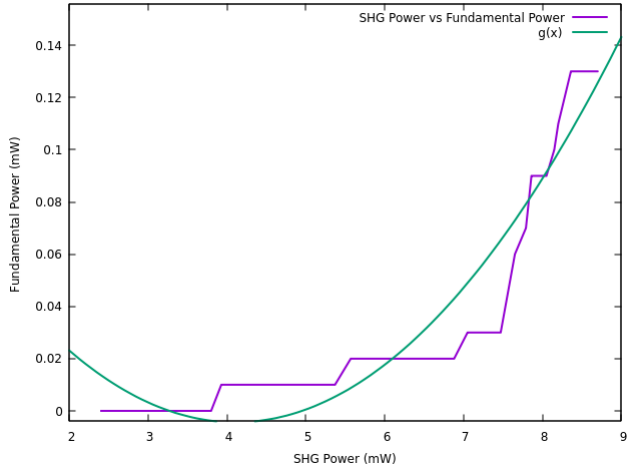


FIG. 23. Output power of SHG as a function of power of fundamental harmonic wave.

It is expected that SHG power varies quadratically with fundamental power. Hence, a quadratic fit  $g(x)$  was performed based on the measured experimental data as shown in fig. 23. Since we could only obtain few datapoints, the original data plot doesn't look exactly quadratic.

Later, we also observed the variation of power output of SHG signal as a function of temperature for various values of injection current. The corresponding data was plotted in fig. 24.

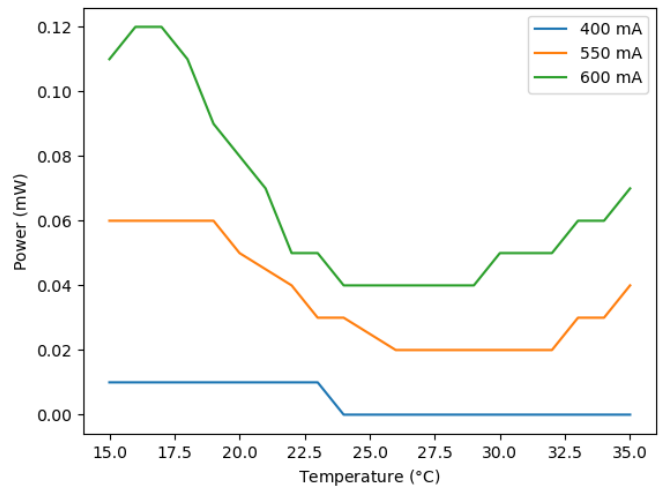


FIG. 24. Output power of SHG as a function of temperature.

From fig. 24, it is observed that the output power achieves maximum value at lower temperatures, with a value going higher with increasing injection current.

#### Q-Switching

Q-switching is an optical technique to achieve fast pulsed beams from a continuous-wave laser system. The details for theory of q-switching were discussed in detail in our pre-midsem report.

The objective was to implement passive q-switching where the saturable absorber used is a Cr:YAG crystal. However, given the provided mechanical holders for the crystal, we were unable to align the lased light (1064 nm) to the central proximity of the Cr:YAG crystal. Although we do obtain a waveform on the oscilloscope as shown in fig. 25, it is however not *q-switched*.

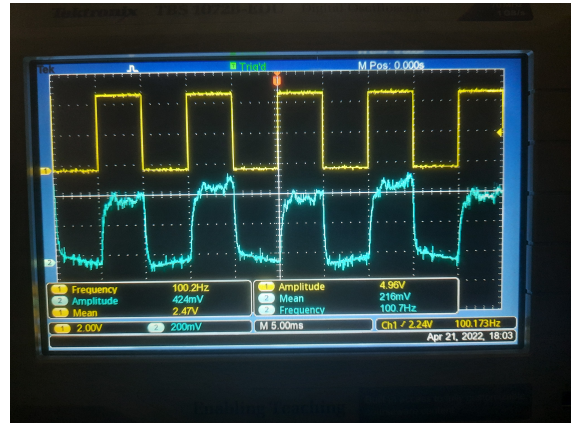


FIG. 25. An unsuccessful attempt to achieve q-switching.

## CONCLUSION

As mentioned earlier, the critical area of dysfunction for the setup is misalignment of the optical components with respect to each other.

## ACKNOWLEDGEMENT